



Influence of a single adatom on sputtering at grazing incidence – A molecular-dynamics case study of 5 keV Ar impact on Pt (111)

Yudi Rosandi^a, Alex Redinger^b, Thomas Michely^b, Herbert M. Urbassek^{a,*}

^aFachbereich Physik, Universität Kaiserslautern, Erwin-Schrödinger-Straße, D-67663 Kaiserslautern, Germany

^bII. Physikalisches Institut, Universität Köln, Zùlpicherstraße 77, D-50937 Köln, Germany

ARTICLE INFO

Article history:

Received 16 March 2008

Accepted for publication 19 November 2008

Available online 6 December 2008

Keywords:

Molecular-dynamics

Ion-solid interactions

Scattering

Channeling

Radiation damage

Sputtering

Surface roughness and topography

Platinum

ABSTRACT

Grazing incidence ion impact on a flat terrace lets the projectile reflect specularly off the surface, leading to little or no damage production or sputtering. The presence of isolated surface defects may change this behaviour drastically. We investigate this phenomenon for the specific case of 5 keV Ar ions impinging at 83° towards the surface normal onto the Pt (111) surface. Molecular-dynamics simulations allow to study the influence of isolated adatoms in detail. The scattering of the projectile from the adatom can redirect the projectile, or let the adatom recoil, such that either of them deposits considerable energy in the target surface, leading to abundant damage production and sputtering. Two distinct collision zones are identified: (i) When the projectile hits the surface in front of the adatom, it may collide with the adatom indirectly (after being specularly reflected off the surface); (ii) alternatively, it may hit the adatom directly. We quantify our results by measuring the zone of influence ($\cong 13 \text{ \AA}^2$) around the adatom, into which the projectile must hit in order to collide with the adatom, and by the sputter cross section of roughly 110 \AA^2 . The data compare well with previous simulation results of sputtering from an atomically rough surface.

© 2008 Elsevier B.V. All rights reserved.

1. Introduction

Grazing-ion incidence on surfaces is interesting both from a fundamental and from an applied point of view [1]. Glancing-ion reflection or channelling along the surface has been used as a means for surface analysis; this technique has brought interesting insight into many aspects of surface science, including electron emission [2], surface magnetism [3], and surface topography [4]. Ion beams at glancing incidence are also used to pattern surfaces, and can induce in particular pronounced ripple structures on the surface [5]. Recently, the application of glancing-ion incidence on nanopatterning of surfaces has been investigated and the detailed atomistic aspects of glancing-ion incidence on surfaces were shown to be relevant for an understanding of the initial stages of pattern formation on metallic surfaces [6].

Flat surfaces reflect ions at specular incidence quite ideally, with only little energy transfer to the surface. As a consequence, little or even no damage is formed on the surface, and no sputtering occurs. However, even slight imperfections of the surface may alter the situation dramatically. Thus a considerable influence of the target temperature on sputtering has been found in this regime

of incidence angles [7]; such a temperature dependence is due to the resulting surface irregularities, which strongly affect the reflection. Monoatomically high surface steps, which separate one terrace from the other, also strongly scatter the incident ion and are hence a source of abundant sputtering and damage formation. The influence of these steps on damage formation, and hence on the onset of pattern formation on the surface, has been analyzed recently [8,6]. Finally, at low temperatures, surfaces may be atomically rough. In a simple model, assuming the atomic roughness to be provided by a random distribution of adatoms, atomic roughness was shown to dramatically increase sputter and damage yields for grazing incidence angles [9]. However, in that investigation, the detailed mechanism, by which this enhancement is produced, could not be resolved.

We note that since the early 1970s, the technique of low-energy ion scattering (LEIS) was used successfully to study the composition and structure of the surface [10–13]. It allowed to measure pre-existing surface defects and also adsorbates [14–17]. This experimental technique is based on an analysis of the fate of the ion after scattering off the surface; for the determination of adsorbate characteristics, also the detection of the recoiling atom (LERS) could be employed [18]. The appropriate theoretical and simulation tool consists therefore in so-called *classical trajectory simulations*, in which the result of the ion impact on the target could be ignored [10,11]. These simulations did not allow to determine

E-mail address: urbassek@hrk.uni-kl.de (H.M. Urbassek).

URL: <http://www.physik.uni-kl.de/urbassek/> (H.M. Urbassek).

the fate of the target due to ion impact; for questions such as the ion-induced damage and sputtering, the interactions among the target atoms need to be included.

In the present paper we wish to study the influence of atomic roughness on sputtering and damage formation in a particularly simple scenario: We put a single adatom on an otherwise flat terrace. The flat terrace is bombarded under conditions, which lead to complete ion reflection without damage formation or sputtering. In this way, the effect of a single adatom on the surface can be isolated, and the mechanisms leading to sputtering and damage formation can be elucidated. In this study, we thus treat the static (low-fluence) limit, and do not investigate the effects of a finite ion fluence on the surface morphology. From a theoretical point of view, our approach is novel, since in the overwhelming majority of sputtering studies, a flat (defect-free) surface is assumed [19–24]. Since in experiment, surfaces usually contain defects, our paper allows to estimate how much a given surface defect density changes the sputter yield of an otherwise nonsputtering surface.

2. Method

2.1. Simulation

We consider the impact of 5 keV Ar atoms on a Pt (111) surface at a fixed incidence angle of 83° towards the surface normal. The incidence azimuth is chosen such that its projection onto the surface is aligned in the $[\bar{1}\bar{1}2]$ direction. These particular parameters are chosen, since they correspond to the situation found in experiments [6]. Our simulation crystallite contains 15 layers; each layer extends 100 \AA in the direction of the ion beam, and is 87 \AA broad. Thus the total number of Pt atoms in the crystallite amounts to 20160. We employ a many-body interaction potential [25] for the Pt–Pt interaction, while the Ar projectile interacts via the purely repulsive ZBL potential [26] with Pt. The simulation is performed at a temperature of 0 K by relaxing the target structure to minimum potential energy and quenching the kinetic energy; it can thus be considered to be representative for a situation where the temperature is so low that adatom diffusion can be neglected.

The adatom is put at a stable fcc site on top of the crystallite. Its position, as well as that of all surface atoms are relaxed. The height of the adatom above the surface is $h = 2.27\text{ \AA}$.

Fig. 1a gives a schematic view of the simulation target. In a first set of simulations, we bombarded this surface randomly, in order to identify the outer bounds of the relevant impact zone, outside of which the sputter yield vanishes. This relevant impact zone is indicated in Fig. 1a; it consists of two rectangular areas of 30 \AA^2 each. In a second set of simulations, we bombarded this impact zone with a number of 1200 ions, which were placed on a regular grid [27] of mesh size 0.5 \AA (along the ion flight direction) $\times 0.1\text{ \AA}$. Each trajectory is followed for 10 ps. This time is sufficient to decide on the fate of the projectile and the adatom, and also to determine the sputter yield reliably. The damage production on the surface, however, may still change after this time due to relaxation and diffusion processes. We are confident, though, that the qualitative features of the damage production may be analyzed already at this time.

For purposes of demonstration, we analyzed with particular care the trajectories of projectile and adatom for a specific set of impact points; these lie on a line along the ion direction, passing the adatom site, cf. Fig. 1a, and are spaced by 0.5 \AA .

We consider all those atoms as sputtered that have zero potential interaction energy with the target; due to our cutoff radius of 5.1 \AA this means that they are a distance of at least 5.1 \AA away from all substrate atoms or adatoms of the target. The damage production will be quantified in the following by counting all those atoms

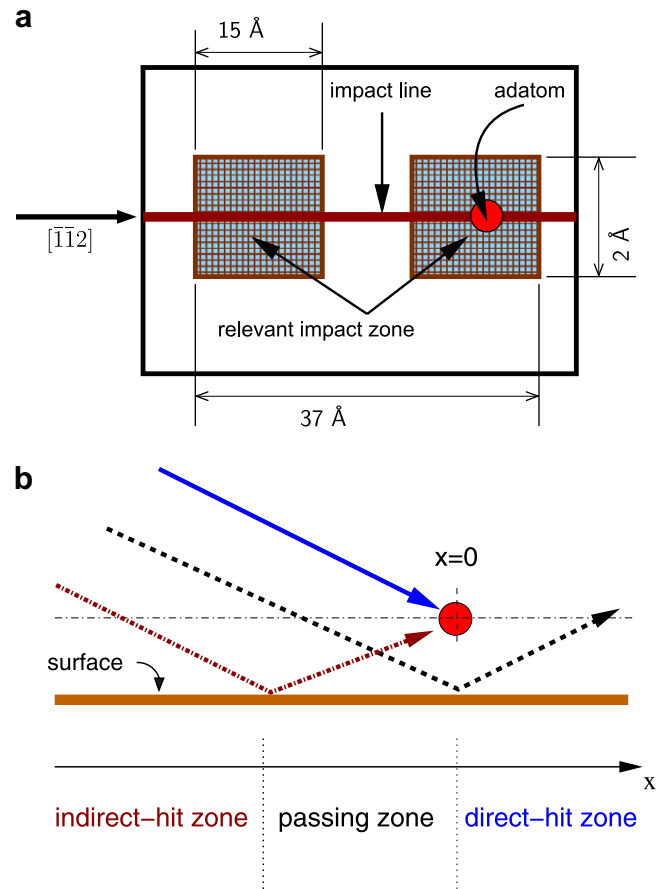


Fig. 1. (a) Schematic view of the Pt (111) surface, covered by an isolated adatom. The impact azimuth $[\bar{1}\bar{1}2]$ and the impact line for central collisions are indicated. While the entire surface was investigated for sputter events, ion impacts on the 'relevant impact zone' were positioned on the fine grid shown. (b) Side view of the Pt (111) surface indicating the indirect-hit, the passing, and the direct-hit zone.

as adatoms, which are above the initial substrate surface; the initial adatom is not included.

In order to assess the effect of temperature on our simulations, we also investigated ion impact on this surface at 90 K. We chose this temperature since at temperatures above 100 K, adatoms become mobile [28]. Velocity scaling is employed to reach this temperature in the target; we let it relax for at least 25 ps to reach equilibrium. For each ion impact, both a novel implementation of the thermally equilibrated crystallite and a new ion impact point were used. 240 ion trajectories were followed for a time of 20 ps each. We note that for these simulations it was essential to fix the bottommost layer of the crystallite in order to stabilize it against 'floppy' long-wavelength vibrational and torsional modes.

2.2. Sputter cross section

In order to define the sputter yield of an inhomogeneous target, we proceed as follows. Assume a target area A is irradiated with a homogeneous fluence ϕ of ions with a total number of ions $N_{\text{ion}} = \phi A$. The (average) total number of sputtered particles N_{sp} will be proportional to the ion fluence. This allows to define a *sputter cross section* via

$$\sigma_{\text{sp}} \phi = N_{\text{sp}}. \quad (1)$$

Hence

$$\sigma_{\text{sp}} = A \frac{N_{\text{sp}}}{N_{\text{ion}}}. \quad (2)$$

This definition is easily implemented in the simulation. Note that this definition requires that in the absence of an adatom, no sputtering occurs; this condition is well fulfilled in the case studied here.

The sputter yield in a homogeneous system is conventionally defined by

$$Y = \frac{N_{sp}}{N_{ion}}. \quad (3)$$

This concept is not helpful in our situation, since – in contrast to the sputter cross section – the sputter yield depends on the total area irradiated, A .

$$Y = \frac{\sigma_{sp}}{A}. \quad (4)$$

However, we can use the concept of a sputter yield in the case of a surface covered *randomly* with adatoms. Then we have a (statistically) homogeneous target, and the concept of a sputter yield applies.

Such a surface is uniquely characterized by the adatom coverage,

$$\Theta = N_{ad} \frac{A_0}{A}, \quad (5)$$

where N_{ad} is the (average) number of adatoms found on an area of size A and $A_0 = 1/n_0 = 6.67 \text{ \AA}^2$ is a measure of the cross sectional area of an atom, where n_0 is the areal density of the surface plane. It can be assumed that $0 \leq \Theta < 1$. The sputter yield in this system is a function of coverage, $Y = Y(\Theta)$, and can be calculated in simulation conveniently by Eq. (3).

For small coverages, $\Theta \ll 1$, it can be assumed that the sputter yield is proportional to the coverage,

$$Y(\Theta) = y_1 \Theta, \quad \Theta \ll 1. \quad (6)$$

We call y_1 the *sputter coefficient* of an adatom. In this situation, the adatoms are so strongly diluted that each sputter event is due to a single adatom, while the existence of all surrounding adatoms can be ignored. Hence, y_1 must be connected to σ_{sp} . Indeed, for a single adatom, $\Theta = A_0/A$; and from the above it follows

$$\sigma_{sp} = AY = Ay_1 \frac{A_0}{A} = y_1 A_0. \quad (7)$$

Thus, y_1 can be regarded as a dimensionless representation of the sputter cross section. We note that our definition of a sputter cross section is equivalent to that used in experimental studies of the ion-induced desorption of adsorbates off a surface, $Y = \Theta n_0 \sigma_{sp}$ [14–16,29].

3. Results

Fig. 1b shows a (schematic) cross sectional view through the surface for the specific set of simulations, in which the impact plane passes the adatom. The ion impact point along this line, measured at the height of the adatom defines the x coordinate. $x = 0$ corresponds to a direct hit with the adatom. Three regions can be distinguished:

1. In the region around $x \cong 0$, the projectile collides directly with the adatom. We call this zone the *direct-hit zone*. Direct hits may both scatter the projectile towards the surface and let the recoiling adatom move towards it.
2. In the middle region, around $x \cong -h \tan \vartheta$, corresponding to 19 \AA in our case, the projectile passes between the adatom and the surface. We call this zone the *passing zone*. In this zone,

the influence of the projectile on the adatom will be minor, and may at most lead to desorption of the adatom, but will leave no traces on the surface.

3. At still larger distances from the adatom, the projectile scatters off the surface and then hits the adatom. This happens in a zone around $x \cong -2h \tan \vartheta$. We call this the *indirect-hit zone*. Indirect hits may lead to backscattering of the projectile towards the surface and may also scatter the adatom to the surface.

3.1. Fate of projectile

Fig. 2 shows the deflection of the projectile as a function of its impact point. The scattering angle is measured in the incidence plane of the projectile with respect to the $[\bar{1}\bar{1}2]$ direction on the surface, i.e., $\vartheta < 90^\circ$ corresponds to forward scattering, $90^\circ < \vartheta < 180^\circ$ corresponds to backward scattering, while $\vartheta > 180^\circ$ corresponds to implantation into the surface. We observe that both in the indirect- and the direct-hit zone, violent collisions occur, which scatter the projectile both in forward and backward directions, and let it also implant into the surface. The energy loss of the projectile is strongly correlated to the deflection angle, such that larger deflections lead to stronger energy losses; a deflection of 90° corresponds roughly to an energy loss of 2–3 keV. Projectile implantation can also occur at impact points of $x \cong -25 \text{ \AA}$ and $x \cong -8 \dots -3 \text{ \AA}$. Analogously to Eq. (2), we can calculate an implantation cross section; it amounts to $\sigma_{\text{implant}} = 2.1 \text{ \AA}^2$.

3.2. Fate of adatom

Fig. 3 assembles data on the fate of the adatom. Due to collision kinematics, the adatom will scatter mostly in the forward direction, $\vartheta < 90^\circ$; for 2-body collisions, as a maximum $\vartheta = 97^\circ$ is possible. Those few adatoms that are scattered by more than 97° suffered further interactions with surface atoms. By the collision, the adatom can receive kinetic energies up to around 3 keV. It will receive the highest energy when hit centrally, and recoils with small scattering angle. There is also a small chance that the adatom is implanted into the target; this happens at $x \cong -34 \dots -30 \text{ \AA}$ and $x \cong +1 \dots +6 \text{ \AA}$, and leads to only moderate implantation depths of around 1.4 \AA , i.e., immediately below the surface layer. Rarely, the adatom is hit under such glancing angles that it receives only

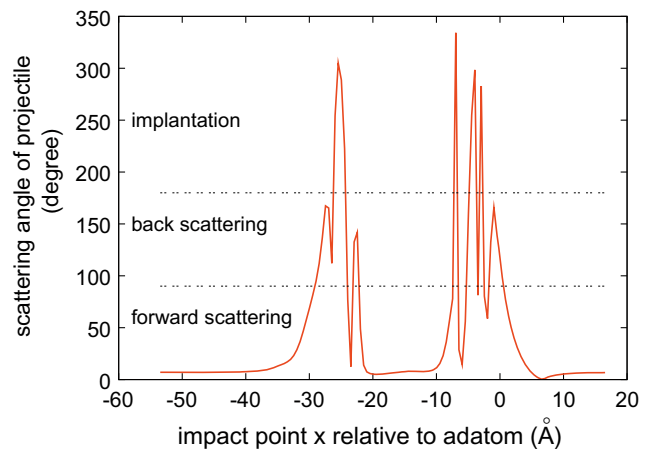


Fig. 2. Scattering angle ϑ of the projectile as a function of the impact point x of the projectile. ϑ is measured in the impact plane with respect to the $[\bar{1}\bar{1}2]$ direction along the surface. The regions of forward and backward scattering, and of implantation into the target are indicated. The coordinate x measures the impact point of the projectile along this direction; $x = 0$ corresponds to a direct hit with the adatom.

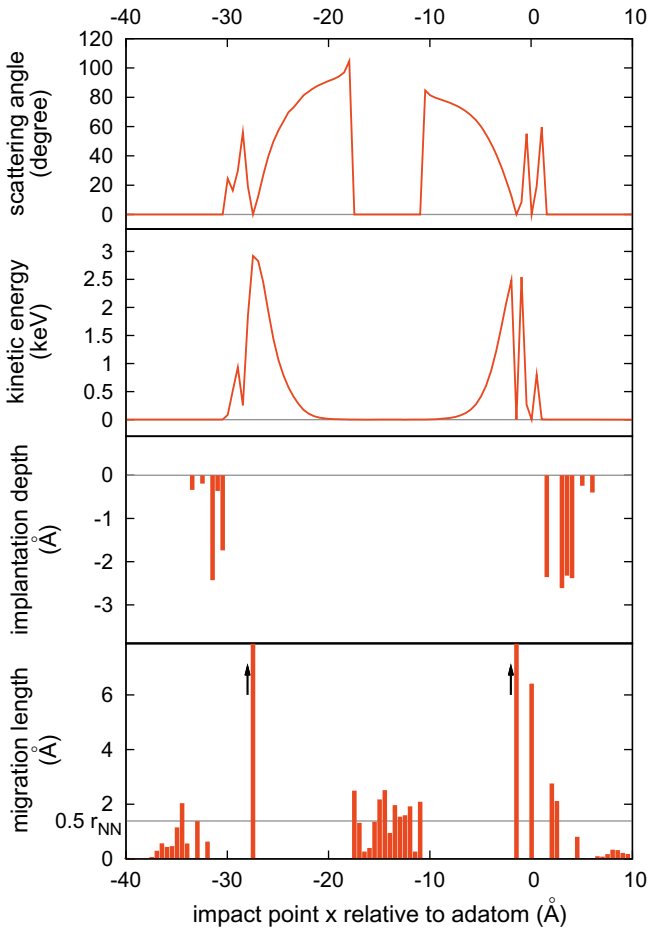


Fig. 3. Scattering characteristics of the adatom as a function of the impact point x . (a) Scattering angle ψ in the impact plane with respect to the $[112]$ azimuth. (b) Kinetic energy. (c) Implantation depth. (d) Migration distance along the surface after 1 ps. Adatoms relocated less than $0.5r_{NN}$, where $r_{NN} = 2.775 \text{ \AA}$ denotes the nearest-neighbour distance in Pt, may return to their original site. The arrows indicate migration lengths $>8 \text{ \AA}$.

momentum parallel to the surface; it is then relocated along the surface, contributing to ion-induced adatom mobility. Since our target is at zero temperature and no electronic losses are included, quite long migration paths on the surface are possible. The migration cross section, defined in analogy to Eq. (1), amounts to $\sigma_{\text{migrate}} = 32.2 \text{ \AA}^2$, while the adatom implantation cross section is 3.85 \AA^2 . The probability that the adatom is desorbed is quantified by the cross section $\sigma_{\text{desorb}} = 22.9 \text{ \AA}^2$.

3.3. Fate of target

The target may respond to the energy input by the reflected projectile or the recoiling adatom by the formation of damage and sputtering. Fig. 4 characterizes the dependence of the sputter and adatom yield on the projectile impact point. Again, the contribution of the direct- and indirect-hit zones are clearly discernible. Sputtering reaches values up to $Y = 20$, while the adatom yields may amount to more than 50 for particular trajectories. Note that we exclude ion-induced desorption of the adatom in counting the sputtering yield.

As outlined in Section 2.2 above, we cannot define the sputter yield of a surface covered by a single adatom. The sputter cross section, Eq. (1), amounts to $\sigma_{\text{sp}} = 110 \text{ \AA}^2$, and the sputter coefficient to $y_1 = 16.5$. The total target sputter cross section, including adatom desorption, thus amounts to 133 \AA^2 .

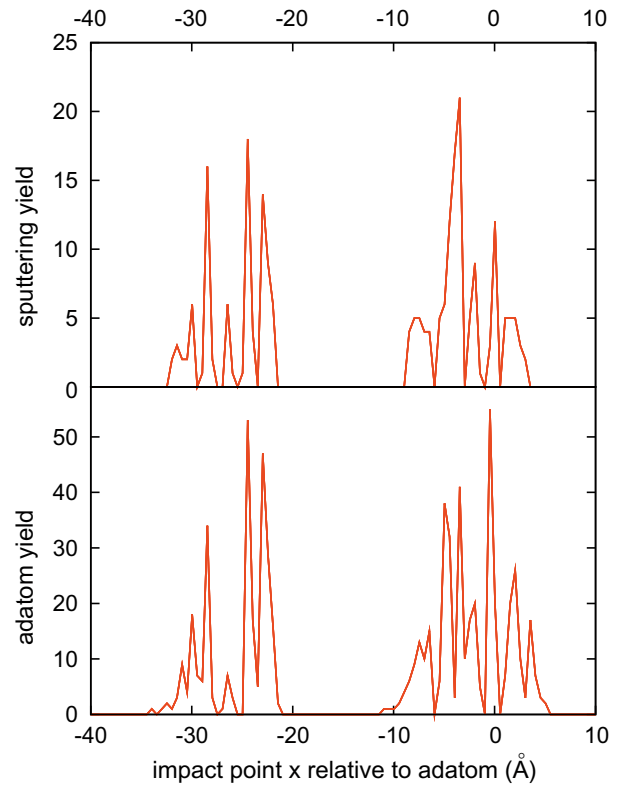


Fig. 4. Sputter yield (a) and adatom yield (b) as a function of the impact point x .

In Fig. 5 we compare this result with published data on the sputtering yield of a surface, which is randomly covered with adatoms [9]. This is possible by extrapolating our present result using Eq. (6) for small values of the coverage Θ , where the effects of the adatoms on the sputtering act independently. Fig. 5 shows that our present results are in good agreement with those obtained for a randomly covered surface. The agreement holds up to a coverage of $\Theta \cong 0.3$; for larger coverages the yield decreases. This is due to the fact that adatoms start shadowing each other so that their influence on sputtering diminishes. For coverages $\Theta \rightarrow 1$, the sputter yield approaches zero, since a new defect-free surface layer has formed.

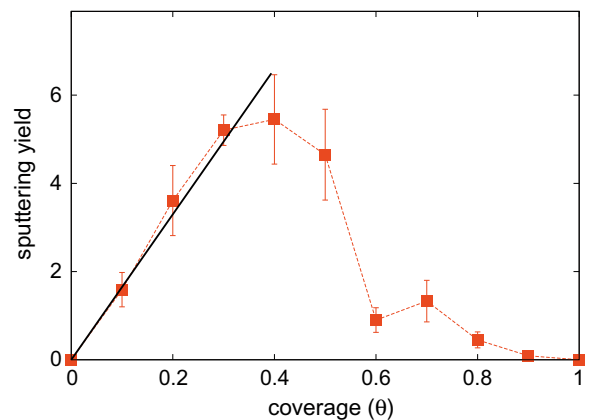


Fig. 5. Comparison of the present simulation data for sputtering of a surface covered with isolated adatoms ($\Theta < 1$) (full straight line) with those of a rough adatom-covered surface ($0.1 \leq \Theta \leq 0.9$) (symbols, connected by line segments) from Ref. [9].

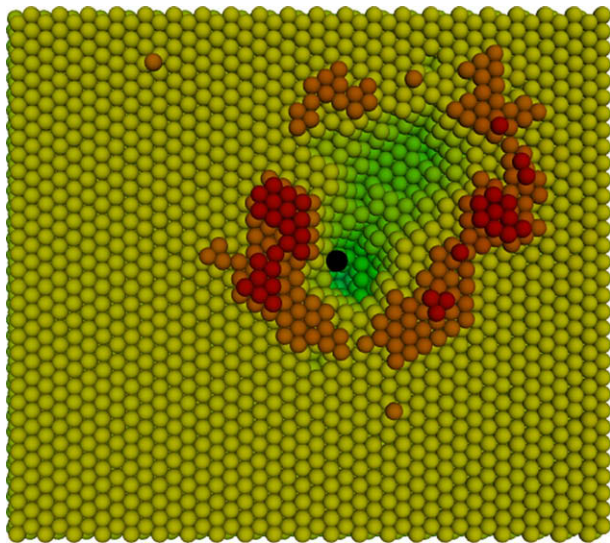


Fig. 6. Top view of damage created on the surface at 20 ps after ion impact. The ion is incident from the left. The original location of the adatom is indicated by a black circle. A case of abundant damage production ($x = -8 \text{ \AA}$) was chosen. Colours denote height above the original surface plane.

Fig. 6 displays a top view of the damage produced in a selected impact event. The formation of a vacancy island surrounded by adatom clusters is seen. We note that we simulated this particular event for 20 ps in order to show the shape of the damage at a time when all spontaneous defect recombination processes have already occurred and the local temperature is so small that no further diffusion is to be expected.

3.4. Zone of influence

Up to now, we analyzed the results of the ion impact only with the help of those selected events whose impact plane passes through the adatom position. For a quantitative discussion, we have to proceed to the analysis of all trajectories.

Fig. 7 shows a contour plot of the sputter yield of all ion impacts in dependence of the (two-dimensional) location of the impact

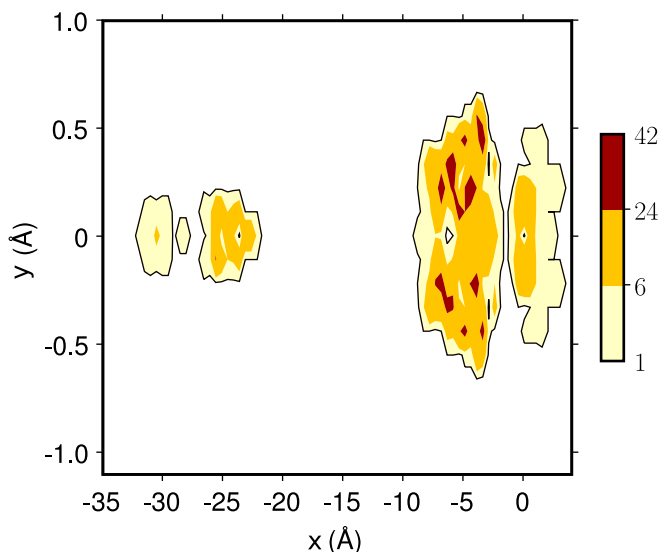


Fig. 7. Contour plot of sputter yield on the Pt (111) surface. The x -axis is directed along $[\bar{1}12]$, the ion flight direction. The adatom was originally at $x = y = 0$. Note the different axis scales in x - and y -direction. The distinction between the indirect-hit zone ($x < -h \tan \vartheta$) and the direct-hit zone ($x > -h \tan \vartheta$) is clearly seen.

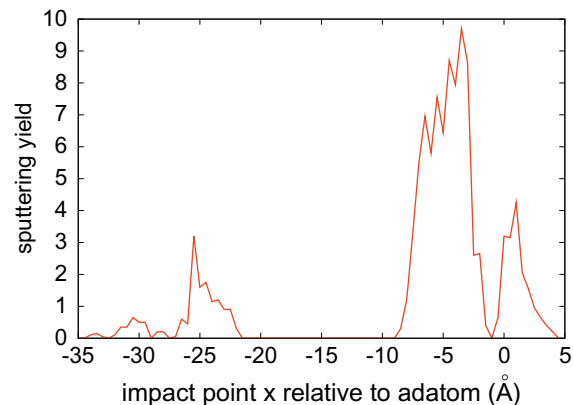


Fig. 8. Laterally averaged sputter yield as a function of the impact point x .

point. The analogous plots for the other quantities studied here look qualitatively similar. Note that the influence of the adatom is localized in two small regions around and in front of the adatom position. These two zones are the indirect- and direct-hit zones mentioned earlier. We may quantify the area of this *zone of influence* by measuring the area, where $Y \neq 0$. This area amounts to 13.1 \AA^2 , here the direct-hit zone contributes 10.45 \AA^2 , while the indirect-hit zone only contributes 2.65 \AA^2 . The direct-hit zone is more productive in the sense that it contributes 86% of the sputtered atoms. The zone of influence is quite small, only around $2A_0$. This small size is consistent with the fact that deviations from the linear behaviour, Eq. (6), only start at $\Theta \cong 1/2$ (more precisely: $1/3$), when the zones of influence start overlapping.

We mention that the average of the sputter yield in the zone of influence amounts to 8.4; however, we doubt that this value corresponds to an experimentally measurable quantity.

Fig. 8 displays the laterally averaged sputter yield. This figure quantifies the fact – already visible in the contour plot, **Fig. 7** – that the indirect-hit zone contributes only little to sputtering, while the direct-hit zone dominates.

3.5. Influence of target temperature

Table 1 summarizes the simulation results on the sputtering cross sections as well as the other cross sections describing the fate of the projectile and of the adatom. We note that the temperature of 90 K amounts to about 40% of the Debye temperature of Pt, 240 K. The influence of thermal vibrations on projectile implantation and on the adatom is minor; hardly any statistically relevant change can be observed.

The sputter cross section has been increased by the thermal motion of the target atoms by around $25 \pm 10\%$. Here the statistical error of our simulation is quite large, due both to our smaller number of simulations performed and to the added thermal fluctua-

Table 1

Cross sections calculated for 5 keV Ar impact on a Pt (111) surface covered with a single adatom. The statistical uncertainty of the projectile and adatom cross sections is mainly given by the number of ions used in the simulation and is estimated as $0.05 (0.5) \text{ \AA}^2$ for the 0 K (90 K) simulation. The uncertainty in the sputter yield also includes fluctuations in the collision cascade induced by the projectile and is indicated in the table.

Process	$\sigma (\text{Å}^2)$ at 0 K	$\sigma (\text{Å}^2)$ at 90 K
Projectile implantation	2.1	1.5
Adatom desorption	22.9	27.5
Adatom migration	32.2	34.5
Adatom implantation	3.85	5.5
Sputtering	110 ± 1.1	138.5 ± 12

tions. A closer inspection of the data shows that this is due to a larger zone of influence which increases from 13.1 \AA^2 (0 K) to 15 \AA^2 (90 K). This result is in qualitative agreement with the increase in sputtering found in Ref. [7] for bombardment of a step. Note that a flat terrace does not sputter under our ion impact conditions even at 550 K.

3.6. Feasibility of an experimental measurement

Although in principle the influence of single atoms on sputtering at grazing incidence could be measured, there are a number of experimental difficulties that rule out a measurement with reasonable precision for the near future. A surface with a small coverage of randomly adsorbed Pt adatoms on Pt(1 1 1) is easy to prepare at temperatures below 100 K, where Pt adatoms are immobile [28]. We could also imagine to collect the sputtered material or to investigate the surface after bombardment by STM to determine the number of sputtered atoms from the amount of surface vacancies after an annealing step. However, each ion interaction with an adatom will change the local situation drastically, causing sputtering, damage creation (adatom-vacancy pairs) or at least adatom relocation. Thus after a very small number of impacts, much less than one ion interaction with each adatom, the surface situation will deviate drastically from the situation initially prepared (compare also Fig. 6). The strong effects of the impinging ions on the situation to be investigated thus forces the experimenter to limit the ion fluence such that the number of ions is much smaller than the number of adsorbed adatoms. For $\Theta \approx 10^{-2}$, e.g., this implies the ion fluence to be smaller than 1×10^{13} ions/cm². Assuming a sputter yield of $Y = 16.5\Theta$, as determined by molecular-dynamics simulation in the present work, this would imply a total number of sputtered atoms of the order of 2×10^{12} atoms/cm². The authors are not aware of a method suitable to measure such small quantities of sputtered material with quantitative precision. Moreover, it will be difficult in praxis to rule out that a significant amount of the counted sputtered atoms is from other surface imperfections like steps (step atoms are always present in a concentration of about 10^{-3}) or adsorbed gas atoms.

The problem of changing the experimental situation severely through ion impacts is of special importance at very low temperatures in the absence of diffusion. At high temperatures, in the presence of diffusion the disturbance of the experimental situation is largely healed between successive impacts. At such high temperatures, however, single atoms are highly mobile, heal to steps and thus cannot be investigated with their effect on sputtering.

The arguments developed here also hold for other defects resulting from the ion-adatom interaction, such as subsurface vacancies or interstitials.

4. Conclusions

We presented a case study of the influence of isolated adatoms on sputtering and damage creation under grazing incidence. The case of 5 keV Ar impact at 83° towards the surface normal on a Pt(1 1 1) surface was chosen, since this system has received considerable interest in the recent past. We find:

1. Whereas impact on a flat terrace creates neither damage nor sputtering, the situation changes drastically by the existence of a single adatom on the surface. The collision of the projectile with the adatom either redirects the projectile, or lets the adatom recoil in a direction, which allows to deposit its energy in the Pt surface, leading to abundant sputtering and damage creation.

2. The mechanism is efficient, leading to sputter yields up to 20 and damage yields above 50. We quantify the effect by calculating the *zone of influence*: impact of the projectile in this zone is influenced by the presence of the adatom. For the case studied its area is roughly 13 \AA^2 . Sputtering is quantified by the *sputter cross section* which is around 110 \AA^2 . In other words, for small adatom coverages, $\Theta \ll 1$, the sputter yield is around $Y = 16.5\Theta$. These findings are in agreement with previous simulations of sputtering of a Pt surface, which is randomly covered with adatoms [9].
3. A detailed analysis of the projectile and adatom trajectories reveals that the zone of influence consists of two disjoint regions: if the projectile hits the surface in front of the adatom, it may hit the adatom indirectly, after being reflected specularly off the surface. The second zone consists of direct hits of the projectile with the adatom. These two zones are separated by a gap, in which the projectile passes between the adatom and the surface, with no or little effect on sputtering and damage production.
4. The dependence of the projectile scattering and implantations, and of the adatom surface migration and desorption could be analyzed in detail in dependence of the projectile impact point.

Acknowledgement

This work has been supported by the *Deutsche Forschungsgemeinschaft*. Y. Rosandi is grateful to a grant from the TPSDP Ministry of National Education, Republic of Indonesia.

References

- [1] H. Winter, Phys. Rep. 367 (2002) 387.
- [2] J. Kirschner, K. Koike, H.P. Oepen, Phys. Rev. Lett. 59 (1987) 2099.
- [3] J. Leuker, H.W. Ortjohann, R. Zimny, H. Winter, Surf. Sci. 388 (1997) 262.
- [4] Y. Fujii, K. Narumi, K. Kimura, M. Mannami, T. Hashimoto, K. Ogawa, F. Ohtani, T. Yoshida, M. Asari, Appl. Phys. Lett. 63 (1993) 2070.
- [5] T. Michely, J. Krug, Islands, mounds, and atoms, Springer Series in Surface Science, vol. 42, Springer, Berlin, 2004.
- [6] H. Hansen, C. Polop, T. Michely, A. Friedrich, H.M. Urbassek, Phys. Rev. Lett. 92 (2004) 246106.
- [7] A. Redinger, Y. Rosandi, H.M. Urbassek, T. Michely, Phys. Rev. B 77 (2008) 195436.
- [8] A. Friedrich, H.M. Urbassek, Surf. Sci. 547 (2003) 315.
- [9] Y. Rosandi, H.M. Urbassek, Surf. Sci. 600 (2006) 1260.
- [10] S.H.A. Begemann, A.L. Boers, Surf. Sci. 30 (1972) 134.
- [11] A.L. Boers, Surf. Sci. 63 (1977) 475.
- [12] H. Niehus, R. Spitzl, Surf. Interface Anal. 17 (1991) 287.
- [13] H.H. Brongersma, M. Draxler, M. de Ridder, P. Bauer, Surf. Sci. Rep. 62 (2007) 63.
- [14] A.G.J. de Wit, R.P.N. Bronckers, T.M. Hupkens, J.M. Fluit, Surf. Sci. 90 (1979) 676.
- [15] J. Onsgaard, W. Heiland, E. Taglauer, Surf. Sci. 99 (1980) 112.
- [16] A.J. Algra, E.P.T.M. Suurmeijer, A.L. Boers, Surf. Sci. 128 (1983) 207.
- [17] B. Poelsema, L.K. Verheij, G. Comsa, Surf. Sci. 148 (1984) 117.
- [18] B.J.J. Koeleman, S.T. de Zwart, A.L. Boers, B. Poelsema, L.K. Verheij, Phys. Rev. Lett. 56 (1986) 1152.
- [19] R. Behrisch (Ed.), Sputtering by Particle Bombardment I, Springer, Berlin, 1981.
- [20] R. Behrisch (Ed.), Sputtering by Particle Bombardment II, Springer, Berlin, 1983.
- [21] R. Behrisch, K. Wittmaack (Eds.), Sputtering by Particle Bombardment III, Springer, Berlin, 1991.
- [22] P. Sigmund (Ed.), Fundamental processes in sputtering of atoms and molecules (SPUT92), Mat. Fys. Medd. Dan. Vid. Selsk., vol. 43, Copenhagen, 1993, entire volume.
- [23] Grove Symposium, Phil. Trans. Roy. Soc. (London) A 362 (1814) (2004) 1.
- [24] R. Behrisch, W. Eckstein (Eds.), Sputtering by particle bombardment, Topics Appl. Physics, vol. 110, Springer, Berlin, 2007.
- [25] H. Gades, H.M. Urbassek, Phys. Rev. B 50 (1994) 11167.
- [26] J.F. Ziegler, J.P. Biersack, U. Littmark, The Stopping and Range of Ions in Solids, Pergamon, New York, 1985.
- [27] T.J. Colla, B. Briehl, H.M. Urbassek, Radiat. Eff. Defects Solids 142 (1997) 415.
- [28] M. Bott, M. Hohage, M. Morgenstern, T. Michely, G. Comsa, Phys. Rev. Lett. 76 (1996) 1304.
- [29] E. Taglauer, Appl. Phys. A 51 (1990) 238.